35th Annual International Conference of the IEEE EMBS
Osaka, Japan, 3 - 7 July, 2013

Dynamic Contrast Enhanced Optical Imaging of Cervix, *in vivo*: A Paradigm for Mapping Neoplasia-Related Parameters*

George Papoutsoglou, *Student Member*, *IEEE*, Theodoros - Marios Giakoumakis and Costas Balas, *Member, IEEE*

***Abstract*—We present a novel biophotonic method and imaging modality for estimating and mapping neoplasia-specific functional and structural parameters of the cervical precancerous epithelium. Estimations were based on experimental data obtained from dynamic contrast-enhanced optical imaging of cervix, *in vivo*. We have developed a pharmacokinetic, *in silico*, model of the optical tracer's uptake by the epithelium. We have identified that the kinetic parameters of the model correlate well with pathologic alterations in both metabolic and structural characteristics of the tissue, associated with the neoplasia progress. Global sensitivity analysis and global optimization methods were employed for identifying the key determinant set of biological parameters that dictate the model's output. Particularly, the shuffled complex evolution algorithm converged to a set of four parameters that can be estimated with an error of 7%, indicating a good accuracy and precision. These results are unique in the sense that for the first time functional and microstructural parameter maps can be estimated and displayed together, thus maximizing the diagnostic information. The quantity and the quality of this information are unattainable by other invasive and non invasive methods.**

I. Introduction

Dynamic Contrast-Enhanced (DCE) imaging is a versatile technique for the spatio-temporal recording of biomarker-induced bio-events and processes in tissues, *in vivo*, non-invasively and in real time. DCE imaging has been established as a non-surgical tool for the study of tissue perfusion kinetics, *in vivo* and has shown an impressive prognostic and predictive capacity in cancer radiology [1]. The concept of DCE is evolving rapidly and has been translated to several biomedical modalities including optical imaging. In fact, the in-vivo optical imaging aspect of DCE (DCE-OI) was developed in late nineties by C. Balas *et al*. [2], [3]. Particularly, a DCE optical imaging method and platform was developed for measuring and mapping the evanescent backscattering signals, generated during the biomarker-tissue interaction with epithelial neoplasias of the cervix, the larynx and the skin [4]. The method employs the acetic acid (AA) dilute solution 3-5% as a biomarker. In two international clinical trials, enrolling hundreds of patients DCE-OI was proved to be very efficient, demonstrating an improvement of more than 63% in diagnostic sensitivity over Papanicolaou test and colposcopy [5].

Due to the fact that DCE-OI captures the kinetics of diffusible, high-affinity labeled tracers in tissues, it, in principle, allows for the model-based estimation of biological parameters that are determining the features of the experimental data. In addition, since DCE-OI measures these data in every spatial location, it enables the mapping of the estimated parameters. To this end, we have previously reported the development of a compartmental model, which simulates the metabolic pathways that are followed by the biomarker in the epithelial tissue [6]. The biomarker uptake kinetics determine the dynamics of the biological target's optical activation and establish the link between optical and biological parameters and responses. Then, fitting the developed pharmacokinetic model to the experimental data, a set of neoplasia-related biological parameters can be estimated, comprising the solution of the inverse problem. Towards this direction, we have performed global sensitivity analysis for ranking the importance and relative estimability of the input parameters [7]. The analysis concluded that four out of nine parameters are fulfilling these criteria and can therefore be estimated using the experimental dynamic optical data as input. These parameters were found to be: the number of neoplastic layers, the size of the extracellular space, the extracellular pH and the tissue porosity.

In this paper we report a method based on global optimization for verifying whether the solution of the inverse problem (a certain set of biological parameter values) is substantially unique. Finally, we for the first time present results from the pixel-by-pixel estimation of these parameters from DCE-OI of cervical tissue, *in vivo*. Four maps have been calculated, having as pixel values the estimated parameter values. The latter are represented in the form of a pseudocolor map which is overlaid onto the clinical color image of the tissue. This enables the direct visualization of tissue locations with normal or abnormal parameter values.

II. Materials and Methods

A. Bio-Optical Background

Chemical biomarkers have been extensively used for visualizing and monitoring several bio-processes at pre-cancer and cancer stages in live cells or tissues. Optical activation of these substances depends primarily on their predefined affinity to cellular components. Still, their uptake

* This work was supported in part by: 1) the European Union (European Social Fund) and Greek National funds through the Operational Program "Education and Lifelong Learning" of the National Strategic Reference Framework–Research Funding Program: Heraclitus II–Investing in knowledge society through the European Social Fund and 2) the NSRF "cooperation" action, program "OncoSeed Diagnostics: Biology of Circulating Tumour Cells, Distant Metastasis & Development of Liquid Biopsy Methods"

C. Balas, G. Papoutsoglou and T. M. Giakoumakis are with the Department of Electronic and Computer Engineering, Technical University of Crete, Chania 73100, Greece (corresponding author to provide phone: +302821037212; fax: +302821037542; e-mail: balas@electronics.tuc.gr).

depends largely on the transport phenomena and pathways that they follow in order to reach and optically activate the target. It is therefore possible to assess valuable information regarding the functional and the structural characteristics of abnormal sites, by studying and simulating, *in silico*, the kinetics of these biomarkers. Towards this end, we have identified and modeled the transport phenomena in the case of the cervical precancerous epithelium using AA as biomarker. Particularly, the AA molecules, after topical application, reach the extracellular space (ES) of the neoplastic portion of the epithelium, where they remain considerably unionized due to the high extracellular acidity. As such, they penetrate passively through the membranes of the neoplastic cells with high selectivity. Due to the almost neutral intracellular space (IS), the intruded AA molecules are disassociated into acetate (Ac^-) and hydrogen (H^+) ions. The latter, stimulate conformational changes in the nuclear proteins. This, in turn, provokes local changes to the index of refraction and determines the macroscopically observed dynamic scattering characteristics. Next, and because the cervical epithelium is stratified, these processes are repeated in the underlying neoplastic epithelial layers. Finally, the tissue restores its original light scattering characteristics by the time the biomarker has been consumed or drained away.

B. Model Formulation and Calibration

Structurally, the cervical epithelium is a natural assemblage of well-differentiated cells which at precancer stages disorganize. Taking normal and pathologic epithelium architecture into the account, we have developed a pharmacokinetic model that encapsulates the abnormal part of the cervical epithelium and partitions it into a stack of functionally and structurally identical cells. Because during the development of neoplasia the number of abnormal cell layers constantly increases, this tissue partitioning has been designed to be flexible in size. This adaptable layered structure is delimited from its upper borders by a reservoir layer that acts as a repository that supplies the biomarker. Each of these cell layers is modeled with two compartments of interaction: the intracellular space (IS) and the extracellular space (ES) compartments. AA diffuses passively from the ES to the IS through the cell's membrane and from the upper to the lower layer(s) of the abnormal epithelium through the extracellular, porous junctions. Both transmembrane and paracellular passive fluxes are driven by concentration and potential gradients, obeying to the Fick's law and Goldman-Hodgkin-Katz flux constant field equation. The model also embodies two dynamic intrinsic processes, the AA ion buffering, occurring in both IS and ES spaces, and the active transmembrane pumping processes, which contribute in restoring the original intracellular pH (pH_{IS}) though the extrusion of H^+ ions from the IS to the ES. For more details the reader is referred to [6], [7].

Altogether, the developed model is a deterministic, non-linear, algorithm that includes a scalable system of coupled differential equations. The differential equation system that expresses material exchange between the compartments of a single neoplastic layer is the following:

$$\dot{\left[\mathrm{TA}\right]}^{i}_{\mathrm{IS}} = a^{-1}J_m^{\mathrm{AA}_i} + a^{-1}J_m^{\mathrm{Ac}^-} \quad (1)$$

$$\dot{\left[\mathrm{H}^+\right]}^{i}_{\mathrm{IS}} = -\ln 10^{\left[\mathrm{H}^+\right]^{i}_{IS}}\left(a\beta_{\mathrm{IS}}\right)^{-1}\left(q^{i}_{\mathrm{IS}}J_m^{\mathrm{AA}_i} - w^{i}_{\mathrm{IS}}J_m^{\mathrm{Ac}_i^-} - J_p^{\mathrm{H}_i^+}\right), \quad (2)$$

$$\dot{\left[\mathrm{TA}\right]}^{i}_{\mathrm{ES}} = b^{-1}J_m^{\mathrm{AA}_i} + b^{-1}J_m^{\mathrm{Ac}_i^-} + a^{-1}\varepsilon J_{\mathrm{T}}^{\mathrm{AA}_i} + a^{-1}\varepsilon J_{\mathrm{T}}^{\mathrm{Ac}_i^-}, \quad (3)$$

$$\dot{\left[\mathrm{H}^+\right]}^{i}_{\mathrm{ES}} = -\ln 10^{\left[\mathrm{H}^+\right]^{i}_{\mathrm{ES}}}\beta_{\mathrm{ES}}{}^{-1}\Big[q^{i}_{\mathrm{ES}}\left(b^{-1}J_m^{\mathrm{AA}_i} + a^{-1}pJ_{\mathrm{T}}^{\mathrm{AA}_i}\right) - w^{i}_{\mathrm{ES}}\left(b^{-1}J_m^{\mathrm{Ac}_i^-} + a^{-1}\varepsilon J_{\mathrm{T}}^{\mathrm{Ac}_i^-}\right) + b^{-1}J_p^{\mathrm{H}_i^+} + a^{-1}\varepsilon J_{\mathrm{T}}^{\mathrm{H}_i^+}\Big], \quad (4)$$

where the brackets ([…]) and the dot (·) denote the concentration time derivative, TA refers to the total AA in both ionized and unionized form, i is the i^{th} neoplastic layer (i=1,2,...,N), a and b are the linear dimensions of the IS and of the ES, where cubic and rectangular compartment geometries have been assumed, respectively, J_m describes the passive transmembrane flux between the ES and IS, β is the buffering power, q and w account for the AA's dynamic ionization constants, including its self-burning effect, ε refers to the alterations in the porosity of the tissue during neoplasia, J_p is the active proton extrusion flux that is assumed to be a piecewise linear function of pH_{IS} and pH_{ES} and J_T is the total passive paracellular flux that corresponds to the difference between the incoming and outgoing molecular paracellular fluxes between consecutive layers through the extracellular porous junctions. It should be noted here that for the reservoir layer equations (3) and (4) are abolished and for the last layer the outgoing paracellular flux is replaced by the $K_V C$ term, where K_V is the permeability at the boundary between the epithelium and the stroma and C corresponds to the concentration of either AA, Ac^- or H^+.

The value ranges of the set of neoplasia related biological parameters as they have been measured experimentally are as follows: the number of dysplastic layers, N, are in the range of 1-10; the IS and the ES linear dimensions a and b, are in the range of 10-20μm and 0.2-0.8μm, respectively; the IS and the ES buffering efficiency β_{IS}, β_{ES}, are in the range of -10 to -50mM and -10 to -30mM, respectively; the pH_{IS}, pH_{ES} values vary between 7-7.4 and 6-7, respectively; the ε parameter is in the range of 1-36 and the K_V between 10^{-6} and 10^{-7} m/s [8-13]. These value ranges comprise the input of the model when fitting of experimental data is intended. A certain combination of parameter values can best-fit the experimental data and therefore be considered, under certain circumstances, as the output of the inverse modeling.

Towards verifying the uniqueness of the inverse problem's solution we have performed consecutively three *in silico* analyses; namely, global sensitivity analysis, parameter identifiability analysis and parameter estimability analysis [7]. On the basis of theses analyses, we were able to decide which of the pertinent model parameters can potentially be estimated from available input/output data and which are impossible to assess. Specifically, we have identified a set of parameters that fulfill the following criteria: a) they are the key determinants of the line-shape of the model's output that fits the experimental dynamic optical data and b) they display no collinearities and minimum interdependency with each other. The initial nine input parameters of the model have been reduced to four by discarding parameter K_V as displaying null sensitivity function and the parameters β_{IS},

β_{ES}, and pH_{IS}, as not fulfilling the combined non-unity correlation coefficient, displaying also low estimability ratio and sensitivity indices. Additionally, the IS linear dimension parameter (a) did not fulfill the collinearity criterion. On the basis of both sensitivity and estimability analyses we have identified that the key determinants (in descending ranking order) are: the number of neoplastic layers (N), the size of the ES (b), the extracellular pH (pH_{ES}) and the tissue's porosity (ε).

C. Solving the Inverse Problem for Parameter Estimation

Even though the implementation of these three analyses enhances the well-posedness of our parameter estimation problem, it does not prove a deterministic relation between the solution and the parameter values. We have identified global optimization methods as the most efficient tool for verifying whether our method has the capacity of providing a substantially unique parameter value combination, when a certain experimental curve is fitted [14]. The first step of the analysis involved the generation of "pseudoexperimental" (PEX) data by collecting the model responses to a known range of values of all four parameters. Next, the PEX curves were fitted until an acceptable level of goodness of fit is reached. At that point a new set of parameters is collected and the procedure is repeated 54 times. Finally, the accuracy and reproducibility of model predicted parameter values was accessed by comparing them with the known PEX values. For implementing this approach we have preliminary employed and tested a series of global estimation techniques that randomly search to converge to the global extrema under a recursive, evolutionary strategy [14]. These methods benefit from the fact that they are easy to implement and not critically dependent on a priori information about the objective function. Under this framework, constrained, direct search, point-to-point and population based, global optimization algorithms such as the simulated annealing, controlled random search, shuffled complex evolution, genetic algorithm and differential evolution, have been comparatively evaluated with the purpose of identifying the best performing algorithm in estimating parameter values in the vicinity of the PEX curve input values, with adequate reproducibility. The normalized root mean squared deviation (NRMSD) was used as convergence/reproducibility metric.

D. Experimental Procedure

Experiment data were obtained from women referred to colposcopy after having an abnormal Pap-test. The DCE-OI head was adapted to a colposcope and a set of 30 images were collected from each case before and after applying AA. The reader can find more details on the image acquisition procedure in [15]. Diffuse reflectance (DR) vs. time curves were calculated for every image pixel, with reflectance values measured at 540 nm (center wavelength), as in this spectral band the signal-to-noise-ratio is maximized. We have selected a case with (biopsy confirmed) high grade cervical neoplasia. From the acquired, in time sequence, image set we have derived 2 million of DR vs. time curves, each corresponding to a single pixel. These curves are one-by-one best fitted and the values of the four parameters are estimated. These four values comprise the pixel values of four maps at the same spatial coordinates. The parameter value-ranges are represented with the aid of a pseudocolor scale and the resulting four pseudocolor maps are overlaid onto the colposcopic image of the tissue. This will, for the first time allow, the clinicians to observe and to localize microstructural and functional alterations, during their routine clinical (macroscopic) examination of the cervix.

III. Results and Discussion

We have found that the best performing algorithm is the shuffled complex evolution (SCE), which converges to solutions of the least NRMSD. The analysis of the factors that may explain the observed differences in the performances between different algorithms goes beyond the scope of this report. For the purposes of current analysis we adopt the SCE algorithm, which gave the results depicted in table I. The results refer to a set of 9 repetitive parameter estimations performed for each PEX signal. It is clear that the chances to convergence to a unique set of parameter values are considerably high, while they vary slightly over the range of the CIN grades. On average, the deviation of the predicted values from the reference ones has been found to be 7% suggesting a high degree of convergence of an almost unique set of parameters' for a given experimental curve. This finding advocates that the estimation of functional and structural parameters can be performed with adequate precision and accuracy.

On the basis on this finding, we claim that the biological parameters that can be estimated through this method from the DCE-OI and the derived DR vs. time curves are realistic and reflect the actual status of the structure and functionality of the tissue. Figure 1(a) shows a DCE-OI image corresponding to a high-grade cervical epithelium (CIN II/III). The circles on this image indicate points from which the biopsy samples were obtained. Figures 1(b)-(e) illustrate the four maps expressing the values ranges and the spatial distribution of the four parameters, calculated for every image pixel. More specifically, fig. 1(b) depicts the spatial distribution of the structural parameter, which expresses the number of neoplastic epithelial layers. As discussed previously, it has been established that the number of neoplastic layers are increasing with the neoplasia growth [8]. By comparing figs. 1(a) and 1(b) it becomes clear that the layer number parameter takes the maximum values (8-10) at the points where the biopsies had been taken, and histology results suggested high occupation of the epithelium by neoplastic layers. This can be reasonably considered as a confirmation of the validity of our results. Fig. 1(c) depicts the spatial distribution of another key structural parameter, which is also assessed histologically as having high predictive value. Parameter (b) expresses the size of the

TABLE I. The precision of the SCE algorithm

Parameter	NRMSD			
	CIN I	CIN II	CIN III	Median
N	9%	9%	4%	9%
b	16%	3%	5%	5%
pH_{ES}	2%	8%	5%	5%
ε	13%	7%	7%	7%

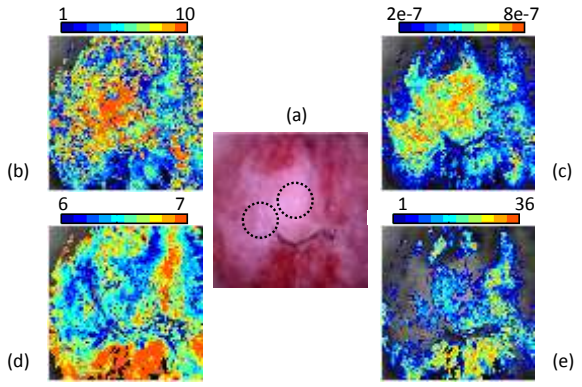

Figure 1. (a) The image of a high risk cervical epithelium. The circles denote the areas from where biopsies have been collected. (b)-(e) Pseudocolor maps of N, b, pH_{ES} and ε neoplasia-related parameters respectivelly, as they have been estimated by our model. Color-coding of the maps corespond to various parameter values.

extracellular space, which is known to increase with the neoplasia progress [8]. As it can be seen in the map of parameter (b), large extracellular spaces exist in the vicinity of the biopsy confirmed high grade points. Additionally, high b-parameter areas are co-localized with the high N-parameter areas, something that can be considered as a verification of the consistency of our findings with the actual biology of neoplasia growth. As it can be seen in fig 1b the number of dysplastic layers is fully consistent with the histological classification and are laying within the nominal value-ranges found in the literature. It is therefore evident that the method presented in this paper may comprise a non-invasive a novel optical biopsy method. Principally, the fact that our approach is based on live tissue imaging makes the assessment of functional characteristics possible, in contrast to histology, which uses dead tissue samples.

Referring now to the functional parameters, our consistency claim applies also to the findings illustrated in fig. 1(d) where areas with high, close to normal, pH_{ES} values are color-coded with red and areas with low pH_{ES}, values with blue. It is distinctly shown that lower pH_{ES} are co-located with high areas with high N and b, depicting the lower acidity of the extracellular space, which is in full agreement with the finding of other studies [11-13]. Finally, fig. 1(e) shows the mapping of the permittivity of the tissue to the biomarker. In general, CIN carcinogenesis disrupts the state of the tissue adhesion structures, which has been associated with increased tissue permeability [16]. This leads to the loosening of these particular junctions, transforming the tissue from tight to leaky increasing the possibility of metastasis. Particularly, according to the "acid-mediated tumor invasion model", the H^+ flow to peritumoral normal tissue provokes normal cell necrosis or apoptosis and extracellular matrix degradation [11]. Because, the tumor cells are capable of resisting to the toxicity induced from this flow, they are able to invade the damaged normal tissue. This allows them to spread, and eventually form invasive cancers. The aforementioned finding suggests strongly that our method can provide a better insight to the neoplasia growth and tumor metastasis.

IV. Conclusion

This paper describes a novel biophotonic method and imaging modality for estimating and mapping a set of neoplasia-related biological parameters, from dynamic optical data (DCE-OI), *in vivo*. Global optimization showed that the estimations of our method are of adequate accuracy and precision. It was also shown that the estimated, in two millions of pixels, values of the four parameters are quite consistent with information provided in the literature. Our findings suggest strongly that our method can improve our understanding of the neoplasia development mechanisms and of tumor growth and metastasis physiology. Corollary, it may become a valuable diagnostic tool that will also facilitate the development and evaluation of new cancer therapies.

References

[1] C. Yue, "The Promise of Dynamic Contrast-Enhanced Imaging in Radiation Therapy," *Sem. Rad. Onc.*, vol. 2, no. 21, pp. 147–156, 2011.

[2] C. Balas, "Methods for characterizing tissues," WO 2008/001037, U.S. Patent P91785US00, 2011.

[3] C. Balas, *et al.*, "In vivo detection and staging of epithelial dysplasias and malignancies based on the quantitative assessment of acetic acid-tissue interaction kinetics," *Jour. Photoch. Photob. B-Biol.*, vol. 53, no. 1–3, pp. 153–157, 1999.

[4] C. Balas, A. Dimoka, I. Orfanudaki and E. Koumantakis, "*In vivo* assessment of acetic acid–cervical tissue interaction using quantitative imaging of back-scattered light: its potential use for the *in vivo* cervical cancer detection grading and mapping," *SPIE-Optical Biopsies and Microscopic Techniques*, vol. 3568, pp. 31-37, 1999.

[5] W. Soutter, *et al*., "Dynamic spectral imaging: improving colposcopy," *Clin. Cancer Res.*, vol. 15, no. 5, pp. 1814–1820, 2009.

[6] C. Balas, G. Papoutsoglou and A. Potirakis, "*In vivo* molecular imaging of cervical neoplasia using acetic acid as biomarker," *IEEE Jour. Sel. Top. Quant. Elect.,* vol. 14, no. 1, pp. 29-42, Jan-Feb, 2008.

[7] G. Papoutsoglou and C. Balas, "Estimation of Neoplasia-Related Biological Parameters through Modeling and Sensitivity Analysis of Optical Molecular Imaging Data", *IEEE Trans Biom Eng*, to be published.

[8] D. Walker *et al.*, "A study of the morphological parameters of cervical squamous epithelium,"*Physiol. Meas.,* vol. 24 pp. 1–15, 2003.

[9] R. Jain,"Transport of molecules across tumor vasculature, " *Cancer Met. Rev.*, vol. 6, pp. 559-593, 1986

[10] P. Swietach, R. D. Vaughan-Jones and A. L. Harris, "Regulation of tumor pH and the role of carbonic anhydrase 9," *Cancer Met. Rev.*, vol. 26, pp 299-310, 2007

[11] P. A. Schornack and R. J. Gillies, "Contributions of cell metabolism and H^+ diffusion to the acidic pH of tumors," *Neoplasia*, vol. 5, no. 2, pp 135-145, 2003.

[12] M. Boyer, M. Barnard, D. Hedley and I. Tannock, "Regulation of intracellular pH in subpopulations of cells derived from spheroids and solid tumours," *Br. Jour. Cancer.*, vol. 68, no. 5, pp 890-897, 1993.

[13] A. Avdeef, "Leakiness and size exclusion of paracellular channels in cultured epithelial cell monolayers-interlaboratory comparison.," *Pharm. Res.*, vol. 27, no. 3, pp. 480–9, Mar. 2010.

[14] G. Papoutsoglou, M. Stamatiadou and C. Balas, "In silico Modeling and Global Optimization of Dynamic Bio-optical Processes for Probing, in vivo, Biological Features of Neoplasia," *in 2012 Conf. Proc. iCBEB Int. Conf.,* pp. 332-335, 28-30 May 2012

[15] C. Balas, "A novel optical imaging method for the early detection, quantitative grading, and mapping of cancerous and precancerous lesions of cervix," *IEEE Trans Biomed Eng,* vol. 48, no. 1, pp. 96-104, Jan. 2001.

[16] G. Sobel, *et al*., "Increased expression of claudins in cervical squamous intraepithelial neoplasia and invasive carcinoma.," *Hum. Pathol.*, vol. 36, no. 2, pp. 162–9, Feb. 2005.